Progress In Electromagnetics Research C, Vol. 89, 39–50, 2019

Two Port Integrated Reconfigurable Microstrip Patch Antenna

Sonia Sharma[1, *], Chandra C. Tripathi[1], and Rahul Rishi[2]

Abstract—A two port, integrated reconfigurable versatile antenna is proposed here. The proposed antenna can reconfigure its frequency, bandwidth, polarization state and radiation pattern and hence is versatile in its characteristics. The antenna is integrated in such a way that the space of one antenna can be used to print two antenna structures to increase the antenna versatility into a small package. PIN diodes are placed in a position so that the electrical switching of the PIN diodes makes every part of the antenna multipurpose. The prototype has been fabricated to authenticate the simulated results. The simulated and measured results are in good agreement. The antenna can be used for Cognitive Radio application.

1. INTRODUCTION

The research area of the antenna designs has become more interesting with the advancements in next generation wireless technology [1–3]. The antenna structure should possess multiple tunable functionalities into a small package. The antenna should optimally utilize its printed space to solve the problem of inefficient large space on the board. Integrated reconfigurable antenna which provides multiple selectable features meets the above said requirement. In [4–18], some design schemes are available in which two antennas are integrated on a solitary substrate to optimize the space utilization. In these reported schemes, small antennas are incorporated in huge sized UWB radiator either by reutilization of large printed area of UWB antenna as ground plane for the second antenna [4–9] or by placing the small sized antenna in electrically neutral area of UWB antenna [10–13]. All these designs are good and solve the problem of underutilization of large printed area of UWB antenna. However in all reported designs, the numbers of reconfigurable features are confined to either frequency reconfiguration or NB-WB reconfiguration [4–18]. However, single reconfiguration feature is not sufficient for future communication devices. Multiple reconfiguration features give the option to select different services in different times using a single and compact antenna structure. Multiple reconfigurabilty features in single antenna add more degree of freedom for emerging technologies. So, different combinations of reconfigurable property increase the capability of supporting multiple standards simultaneously for multi-mode communication.

In this paper, integration concept is extended to design an advanced antenna structure. The proposed antenna structure is incorporated with two elements: a UWB monopole and a versatile reconfigurable antenna as shown in Fig. 1. The U-shape structure on bottom layer which is excited by port[1] is used as UWB antenna from 1–12 GHz. A reconfigurable antenna is printed on the top layer and excited by port[2]. For space management, the big metal area of UWB antenna is reused as ground plane for reconfigurable antenna, and the partially etched ground area of UWB antenna is reused as a printing space for reconfigurable antenna. The proposed integrated antenna is versatile in nature as it can reconfigure its frequency, bandwidth, polarization state and radiation pattern. Now, the user

Received 9 October 2018, Accepted 3 December 2018, Scheduled 14 December 2018

* Corresponding author: Sonia Sharma (sonia990@gmail.com).

[1] Department of Electronics and Communication Engineering, University Institute of Engineering and Technology, Kurukshetra University, Kurukshetra 136119, India. [2] Department of Computer Science and Engineering, University Institute of Engineering and Technology, Maharshi Dayanand University, Rohtak 124001, India.

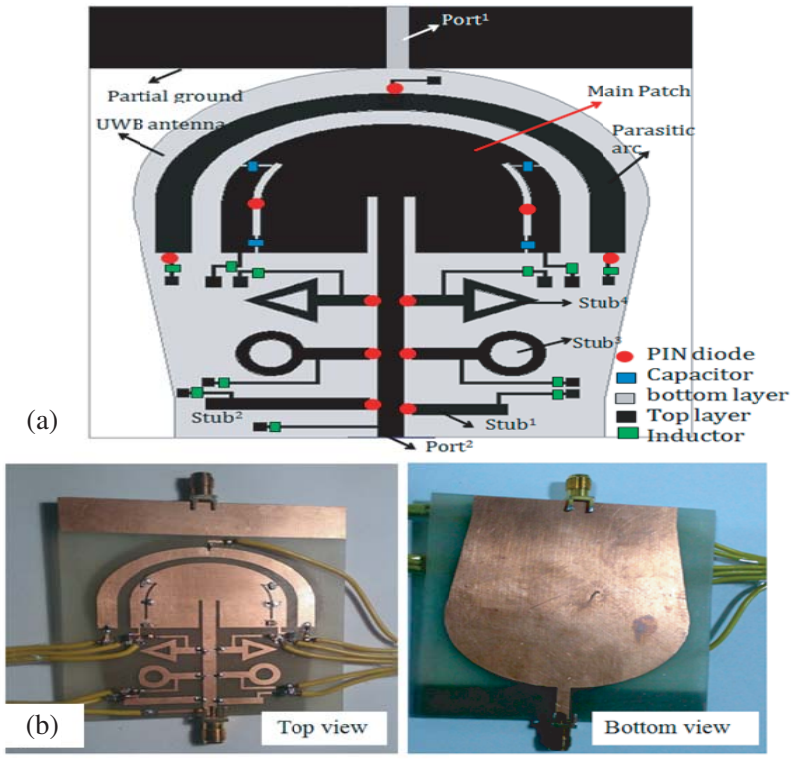

Figure 1. (a) Architecture of proposed two port integrated versatile antenna, (b) fabricated prototype.

can take more than one benefit of any combinations of frequency, polarization, pattern, bandwidth in a single antenna. The tough job in this work is to add multiple reconfigurable features in small printed area. The proposed antenna is integrated in a way that the printed area of one antenna can be used to print two or more antennas for the maximum uses of the available area without disturbing the operating characteristics. The complete design strategy and design evolution of proposed antenna is explained in the next section.

2. DESIGN EVOLUTION

A two port antenna is proposed here in which a UWB antenna is printed on bottom layer. RF signal is applied to it via port[1], and on the top layer a versatile reconfigurable antenna is printed. The versatile reconfigurable antenna is fed by port[1], and it can reconfigure its frequency, bandwidth, and polarization state and radiation pattern. The corresponding antenna topology and its fabricated photograph are shown in Figs. 1(a)–(b). As the two antennas are designed on the opposite sides of the substrate and excited by different ports in different times, there is less interaction between the two antennas. The design steps and strategy adopted for complete design evolution are enlightened here.

At first, a U-shaped radiator is designed on a $7.7 * 7\,\text{cm}^2$ substrate as shown in Fig. 2(a). The U-shaped structure is excited by microstrip feed, and UWB characteristics are confirmed by partially etching the ground plane. The impedance matching is performed by shaping the radiator and controlling the partial ground plane size. Fig. 2(b) shows the variation in partially etched ground plane size on S_{11} characteristics. From the results it is concluded that the RL characteristics are improved in UWB range as the size of partially etched ground plane is increased from 7 mm to 11 mm. But after that, with further increase in the size of partial ground plane, the RL characteristics starts degrading in UWB range. So the optimized size of partial etched ground plane is taken as 11 mm. The geometrical parameters of UWB antenna are $L_s * W_s = 77 * 70\,\text{mm}$, $L_u * W_u = 66 * 60\,\text{mm}$, $L_{gd} * W_{gd} = 11 * 70\,\text{mm}$, $L_{\text{feed}} * W_{\text{feed}} = 11 * 3\,\text{mm}$.

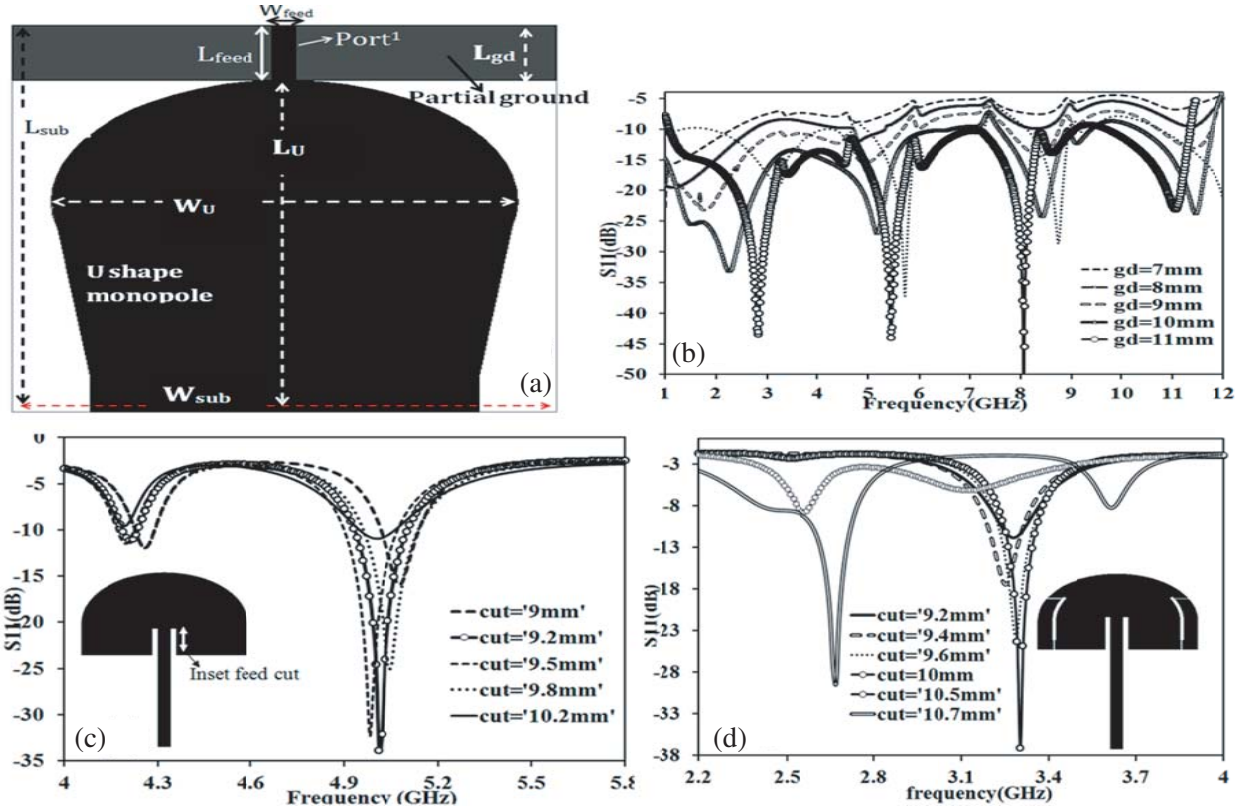

Figure 2. (a) Architecture of UWB monopole, (b) effect of partially etched ground plane size (L_{gd}) and effect of inset cut length in (c) simple antenna, (d) modified antenna.

Now, to design the versatile reconfigurable antenna on the opposite side of UWB antenna, first of all, an inverted U-shaped patch antenna is designed at 5 GHz. This antenna shares the huge printed area of UWB monopole antenna as its own ground plane. So, the two antennas are integrated on a single substrate by sharing its printed area. This antenna is fed by standard 50 ohm microstrip line, and inset cut feeding mechanism is used to tune the antenna. To match the antenna exactly at 50 ohm point, parametric study is done on inset cut length. Fig. 2(c) shows the effect on parameter S_{11} by varying the feed-cut length, and the best value of S_{11} is observed at 5 GHz when the inset cut length is 9.2 mm. In the next design step, two slots are etched on the two opposite edges of the inverted Ushaped patch. But in doing so, frequency, as well as S_{11} parameter of antenna, is affected because of the shift in 50 ohm impedance point. Now, the shifted resonant frequency is 3.26 GHz with return loss value = 13 dB. So, optimization should be done on inset cut length to tune the frequency with better impedance matching. Fig. 2(d) shows the effect on S_{11} parameter by varying the feed-cut length of modified antenna structure, and the results show that the best observed value of S_{11} is 38 dB at 3.26 GHz corresponding to the feed-cut length = 10 mm.

Further, to achieve the frequency reconfiguration in the proposed antenna, four microstrip stubs are accurately positioned in such a way that these matching stubs match the antenna's input impedance at particular frequency as shown in Fig. 3(a). By controlling the activation of different stubs using PIN diodes, shifts in resonant frequency can be controlled. Firstly, the input impedance is calculated from the simulations at the center frequency 3.26 GHz, and this calculated impedance is shifted along the 50 Ω feed line to the location where the input impedance has a real part of 50 Ω and a random imaginary part. At this point ('A'), microstrip Stub^1 is situated parallel to the feed line to cancel the imaginary part. The rectangular Stub^1 tunes the resonant frequency at 4.52 GHz. Here, fine tuning of frequency and RL is done by optimizing the length of Stub^1 (L_1). Fig. 3(b) shows the effect of variation of L_1 on parameter S_{11}, and the optimized length L_1 is 19 mm. Now, to match the antenna at the second frequency, the impedance at the input port is determined so that the antenna can be optimally matched

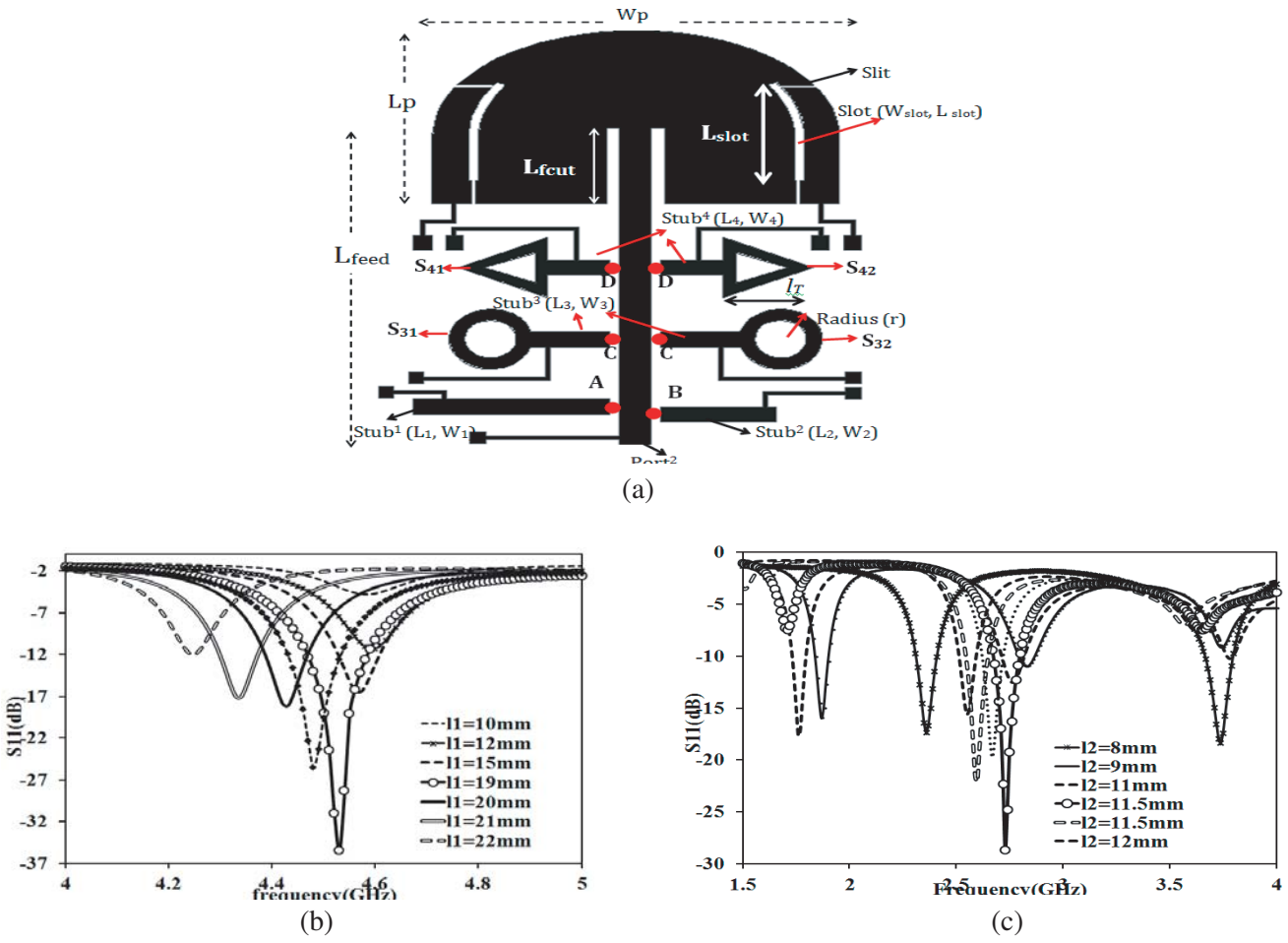

Figure 3. (a) Geometry of versatile reconfigurable antenna, (b) effect of variation in length of stub^1, (c) effect of variation in length of stub^2.

at 2.76 GHz using Stub^2. The rectangular Stub^2 is designed and optimized for 2.76 GHz. Fig. 3(c) shows the effect of variation of L_2 (length of Stub^2) on S_{11} parameter, and the optimized length (L_2) is 11.5 mm.

The geometry of Stub^3 is specially designed to acquire more degree of freedom for the optimization of the resonant frequency. The shape for Stub^3 consists of a rectangular stub and a circular ring attached to its open end. This structure is symmetrically placed across the feed-line at point 'C', and the arrangement of these two structures (S_{31} and S_{32}) is collectively named as Stub^3. To tune the resonant frequency of proposed antenna using Stub^3, initially optimization is done on the position and length of rectangular stub. Fig. 4(a) shows the effect on S_{11} parameter by varying the position of Stub^3. It is observed that for position = 26.8 mm, the resonant frequency is 2.5 GHz, but observed RL is not so good for it. So, further optimization in geometry of Stub^3 needs to be done. This optimization is done by varying the radius of circular ring. Fig. 4(b) shows the effect on S_{11} by varying the radius of circular ring. The final optimized geometry for Stub^3 to tune the antenna at 4.1 GHz is $L_3 = 7.62$ mm, $W_3 = 3$ mm, $R = 4$ mm. Finally, the antenna is tuned at 2.46 GHz using Stub^4. The architecture of Stub^4 is chosen using the same design consideration of Stub^3, but this time triangular ring is designed at the open end of the rectangular stub. Again, we get two degrees of freedom (position and length of triangular ring) to optimize the resonant frequency. The shape for Stub^4 consists of a rectangular stub and a triangular ring attached to its open end. This structure is symmetrically placed across the feed-line at point 'D', and the arrangement of these two structures (S_{41} and S_{42}) is collectively named as Stub^4. To tune the resonant frequency of proposed antenna using Stub^4, initial optimization is done

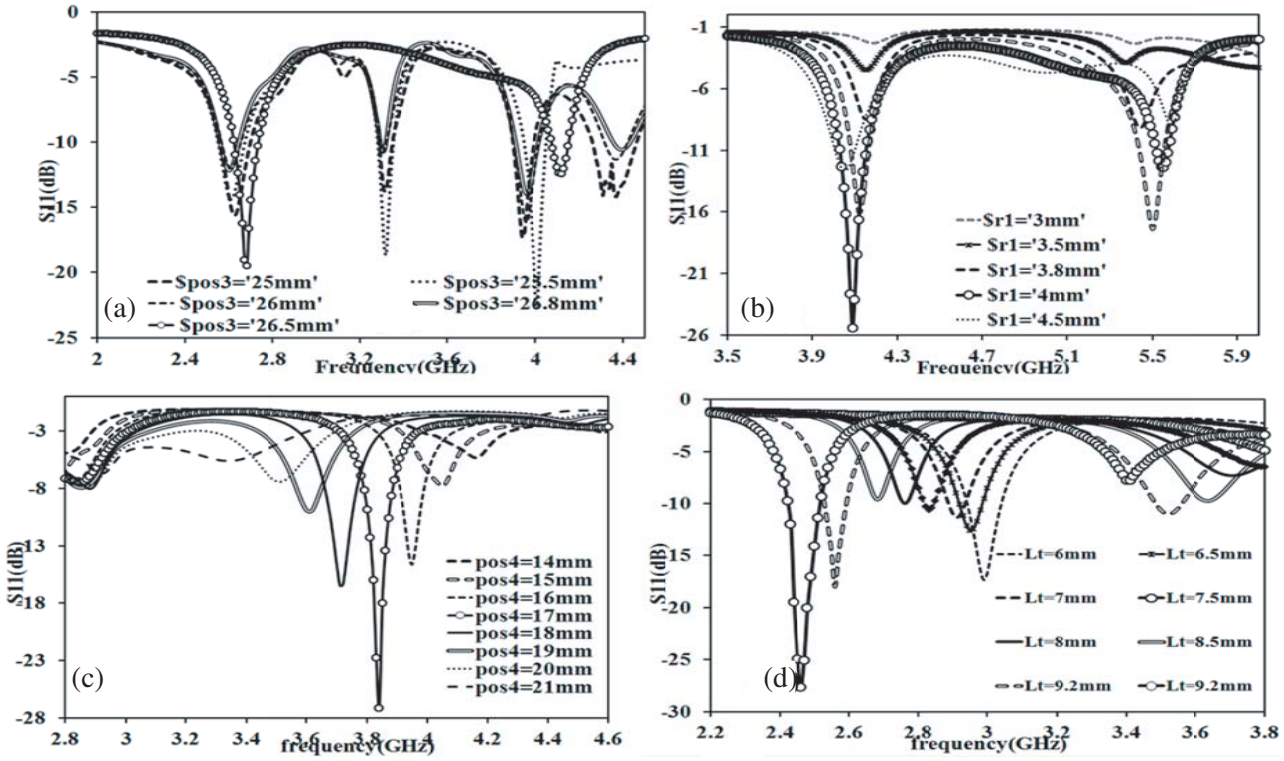

Figure 4. Effect of variation in the (a), (b) position and radius of Stub[3] and (c), (d) position and length of triangular ring of Stub[4].

on the location and length of rectangular stub. Fig. 4(c) shows the effect on parameter S_{11} by varying the position of Stub[4]. After optimization, it is observed that the shifted resonant frequency is repeated (Case[1]), so further optimization in geometry of Stub should be done. For this two triangular rings are added at two corners of Stub[4], and frequency tuning is done by varying the length of triangular ring (l_t). Fig. 4(d) shows the effect on S_{11} parameter by varying the length of triangular ring l_t. After optimization antenna resonates at 2.46 GHz with RL = 26 dB. The final optimized geometry for Stub[4] is $L_4 = 6$ mm, $W_4 = 3$ mm, $l_T = 9.2$ mm.

3. WORKING OPERATION AND RESULT DISCUSSION

The integrated versatile antenna can reconfigure its characteristics in various modes, and active state of all elements for all operating modes is given in Table 1. The prototype for proposed antenna is fabricated, and results for each operating mode are verified in this section. MITS PCB Prototyping Machine is used for the fabrication of proposed integrated antenna. In the fabricated prototype Coil

Table 1. Active part in different operating modes.

Operating mode	Active part	Diode/port condition	Operating freq.
UWB mode	U shape	Port[1]	1–12 GHz
Frequency Reconf. mode	Main patch + Stub[1] to Stub[4]	D_1–D_6, Port[2]	1–6 GHz
Polarization Reconf. mode	Main patch + Stub[1]	D_1, D_7, D_8, Port[2]	3.26 GHz
Bandwidth Reconf. mode	UWB monopole/main patch + Stubs	Port[1]/Port[2]	1–12/1–6 GHz
Pattern Reconfig. mode	Main patch + parasitic arc	D_9, D_10, Port[2]	3.26 GHz

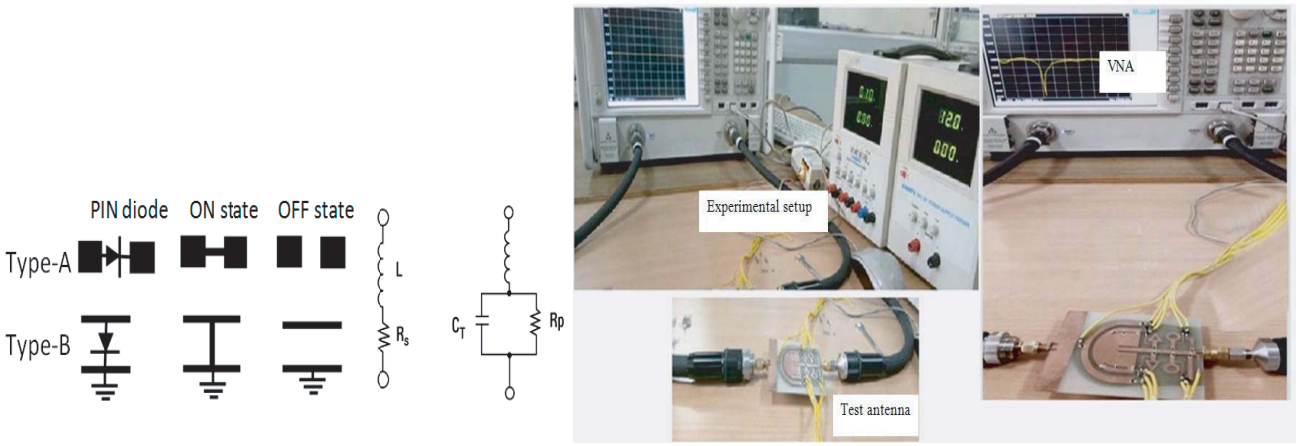

Figure 5. PIN diode switch equivalent circuit in (a) ideal case, (b) practical case, (c) fabricated prototype and experimental setup for integrated versatile antenna.

Craft Inductors, Murata SMD Ceramic Multilayer Capacitors, Infineon BAR64-02 PIN diodes are used. In the proposed design, BAR 64-02 PIN diodes are used as an RF switch to manage the flow of RF signal through different parts of the structure.

Figure 5(a) shows the equivalent model of ideal PIN diode which exhibits zero resistance to current flow in the ON state and infinite resistance to current flow in the OFF state. So, it can be used to open and close the connection between two metal strips on a single layer (Type-A) or between two layers (Type-B) as shown in Fig. 5(a). The equivalent model of PIN diode in forward bias and reverse bias is given in Fig. 5(b). In forward bias PIN diode can be replaced by a 2.1 Ω resistance and 0.6 μH inductance values, and in reverse bias it can be replaced by a 3 kΩ reverse parallel resistance and 0.17 pF capacitance. Ansoft HFSS simulator is used to simulate the structure in which lumped RLC boundary is used to model the equivalent circuit of PIN diode. S parameters of the proposed antenna are measured using Agilent N5222A VNA. The fabricated prototype and measurement setup are shown in Fig. 5(c).

The radiation pattern of the antenna is calibrated in an anechoic chamber using a standard horn antenna. The proposed integrated antenna AUT (antenna under test) is used as receive antenna and placed on the positioner with required elevation and azimuth coverage. Different radiation patterns in xy-plane and xz-plane are measured by switching the short position on parasitic ring manually. To reconfigure the short position high resistivity nichrome wires are used to interconnect portable DC power battery and DC bias pad on AUT. These high resistivity wires reduce the current flow in the transmission lines to avoid reradiation and messing up radiation patterns of antenna. Also portable DC power battery is covered with microwave absorber to mitigate the unwanted effect on the radiation pattern. The transmitted and received powers are measured to calculate the gain of AUT using Friis formula.

The step by step design strategy and working operation for achieving the desired objectives of frequency, polarization, bandwidth and radiation pattern reconfigurability in a single antenna is explained below.

3.1. UWB Mode

For UWB characteristics, the proposed integrated antenna is excited by port[1], and its observed response is shown in Fig. 6(a). From return loss characteristics it is observed that the simulated and measured S_{11} are better than 14 dB in the entire UWB range. The magnitude E field distribution on U-shape antenna at 5 GHz is shown in Fig. 6(b). It is observed that the magnitude of E-field is very large on the outer edge and near the feeding point of U-shape antenna. Simulated value of gain is 5 dB at 5 GHz in UWB range as shown in Fig. 6(c). The shape of gain pattern is omnidirectional for $\phi = 0^\circ$ plane, hence it can sense the spectrum in all directions.

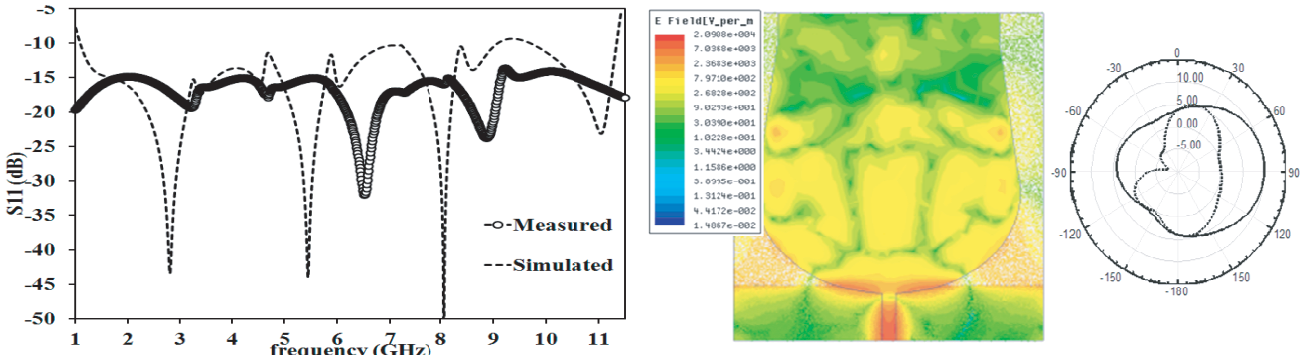

Figure 6. (a) S_{11} vs. frequency in UWB mode, (b) E field distribution, (c) gain pattern in UWB mode at 5 GHz.

3.2. Frequency Reconfigurable Mode

In frequency reconfigurable mode, antenna can switch its resonant frequency by connecting or disconnecting different stubs electronically. These stubs are specially designed for frequency reconfiguration already explained in the previous section. Six PIN diode switches are used to manage the coordination of different stubs independently with the main patch antenna. In this mode, feeding area is mainly designed for frequency switching. Fig. 7(a) shows the feeding area of versatile antenna to understand the biasing scheme for diodes. The feeding structure is composed of four stubs (S_1, S_2, S_3, S_4), 6 PIN Diodes (D_1, D_2, D_3, D_4, D_5, D_6) and DC pads (V_1, V_2, V_3, V_4, V_5, V_6, V_{gd}). The positioning of all PIN switches is done in such a way that they share solitary DC ground pad. The individual PIN switches are activated by providing +5 V on their relevant DC pad and ground signal on V_{gd} DC pad. The PIN diodes control the flow of RF signal entirely through different parts of the feeding structure. Different cases for different combinations of these switches are studied, and certain cases where repeated frequency is obtained have been discarded leaving behind a total of five cases that exhibit desirable results for independent frequency reconfigurable control. Fig. 7(b) shows the active diode and symbolic view of active part of the feeding area under different cases. The direction of RF signal is completely controlled by PIN diodes to reconfigure the antenna's resonant frequency.

The observed and measured S_{11} vs. frequency for all the cases are shown in Fig. 7(c). In case[1], when all diodes are OFF, measured value of RL is 28 dB at 3.32 GHz as compared to the simulated value of 38 dB at 3.26 GHz. For case[2], when Stub[1] is selected by forward biasing the diode D_1, in measurement, the antenna resonates at 4.45 GHz as compared to simulated frequency of 4.52 GHz. The measured value of RL = 35 dB as compared to simulated value of 35 dB. For case[3], when Stub[2] is selected by activating the diode D_2, the proposed antenna resonates at 2.8 GHz. For this case, simulated value of resonating frequency is 2.8 GHz with RL = 22 dB whereas measured value of frequency is found at 2.86 GHz with RL = 24 dB. In case[4], diodes D_3 and D_4 are forward biased to select Stub[3] by applying 5 V on V_3 and V_4 pads. For this case, simulated value of frequency is found at 4.1 GHz with RL value 25 dB whereas measured resonant frequency is found at 4.14 GHz with RL = 22.2 dB. For the last case, Stub[4] is selected when diodes D_5 and D_6 are forward biased by applying +5 V on V_5 and V_6 pads. In this case, simulated frequency 2.46 GHz shows the RL = 28 dB whereas measured frequency 2.41 GHz shows the RL value = 24 dB. In all the cases, measured results are satisfactory; however, frequency shift w.r.t simulated results are attributed to variation in PIN diodes OFF state capacitance w.r.t to frequency in addition to minor fabrication errors. The electric field distributions for all the cases are also shown in Fig. 7(d), and it is revealed that maximum E field is found under the active area of proposed antenna in each case.

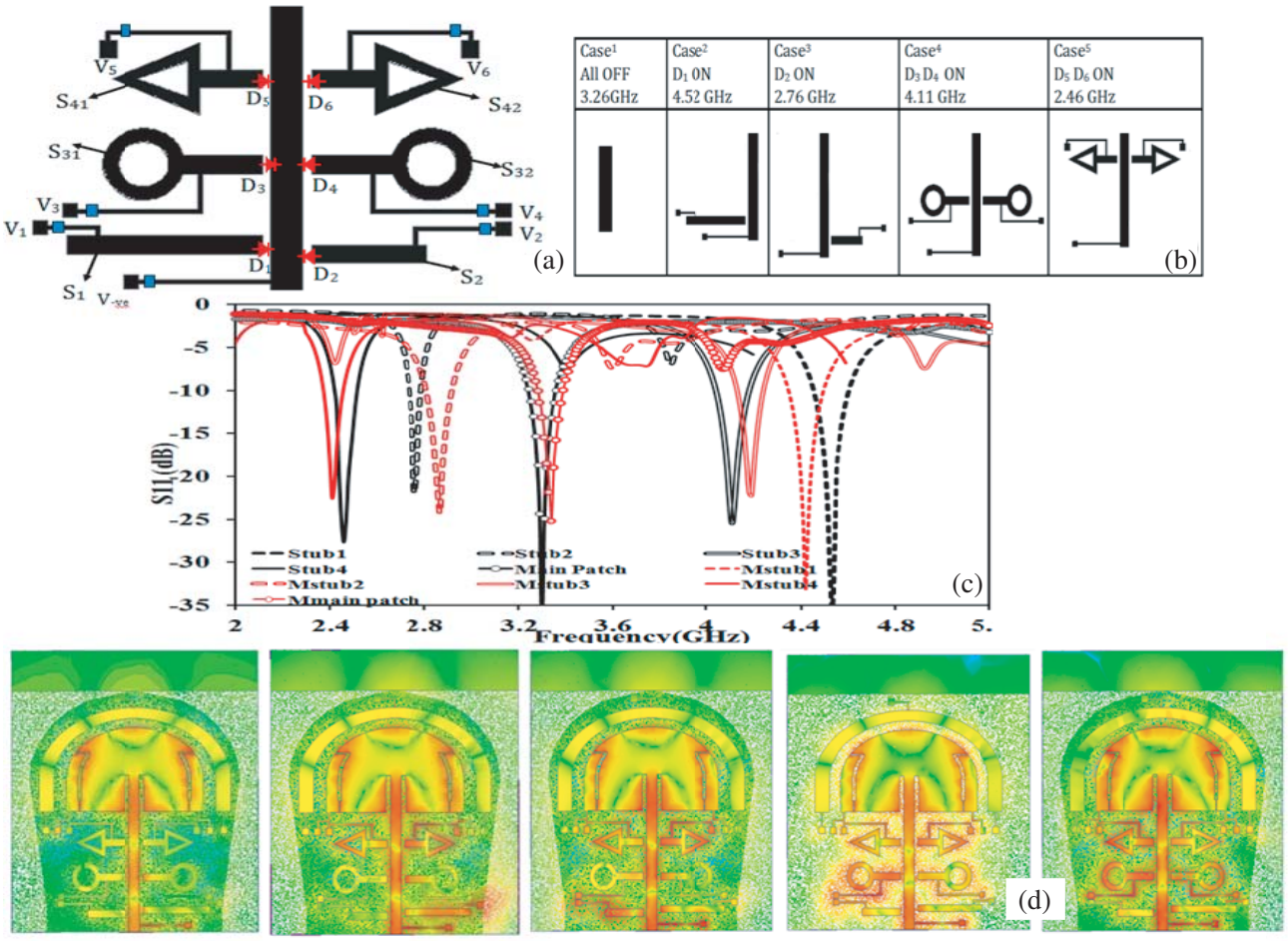

Figure 7. (a) Diode orientation and biasing network, (b) active area of feeding network under different cases, (c) simulated and measured S_{11} vs. frequency, (d) E-field distribution from case[1]–case[5].

3.3. Polarization Reconfigurable Mode

Figure 8 shows the active part of versatile antenna when being operated in polarization reconfiguration mode. To change polarization states, diodes D_7 and D_8 are controlled electronically which are placed inside the slot. When both diodes (D_7 and D_8) are in OFF state, the main patch has a symmetrical structure, thereby producing linear polarization. When one of the diodes, D_7 or D_8, is forward biased, the structure of the main patch becomes asymmetrical. In this case, asymmetrical slot generates two orthogonal modes, thereby producing Circular Polarization (CP) wave. The dimensions of modified cross-shaped slots are $W_{\text{slot}} = 1.5\,\text{mm}$, $L_{\text{slot}} = 12.6\,\text{mm}$. The thin slits of 0.2 mm wide are etched in the circular patch and divide it into three, R, R_1, R_2, isolated regions. By placing 4 SMD capacitors over these slits, ensure the RF continuity and DC isolation between these regions. These DC isolated regions help to bias diodes D_7 and D_8 independently. PIN diode D_7 is activated by providing +5 V on DC bias pad V_7 and ground signal on DC bias pad V_{gd}. Similarly PIN diode D_8 is activated by providing +5 V on DC bias pad V_8 and ground signal on DC bias pad V_{gd}.

In this mode, antenna can switch its polarization state over two frequency bands, i.e., 3.26 GHz and 4.52 GHz. For the first case (Case-A 3.26 GHz), only the main patch is activated, and for the second case (Case-B 4.52 GHz), the circular antenna connected with Stub[1] is activated by forward biasing the diode D_1. The antenna's CP behavior is also analyzed under different stubs combinations, but it is observed that in simulation, axial ratio is not good for Stub[2] and Stub[3], so they are not discussed here. Fig. 9(a) shows the comparison of simulated and measured RL characteristics, and Fig. 9(b) shows comparison of

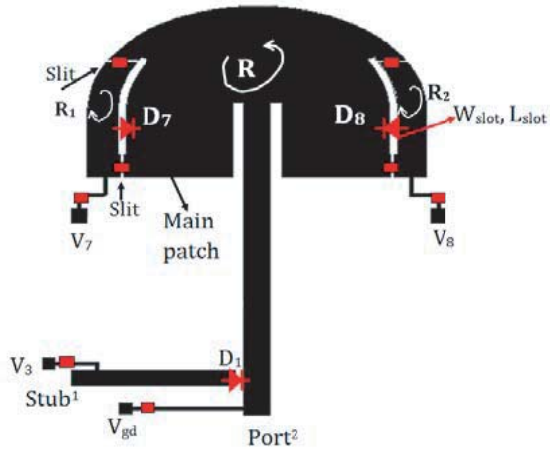

Figure 8. Active area in polarization reconfiguration mode.

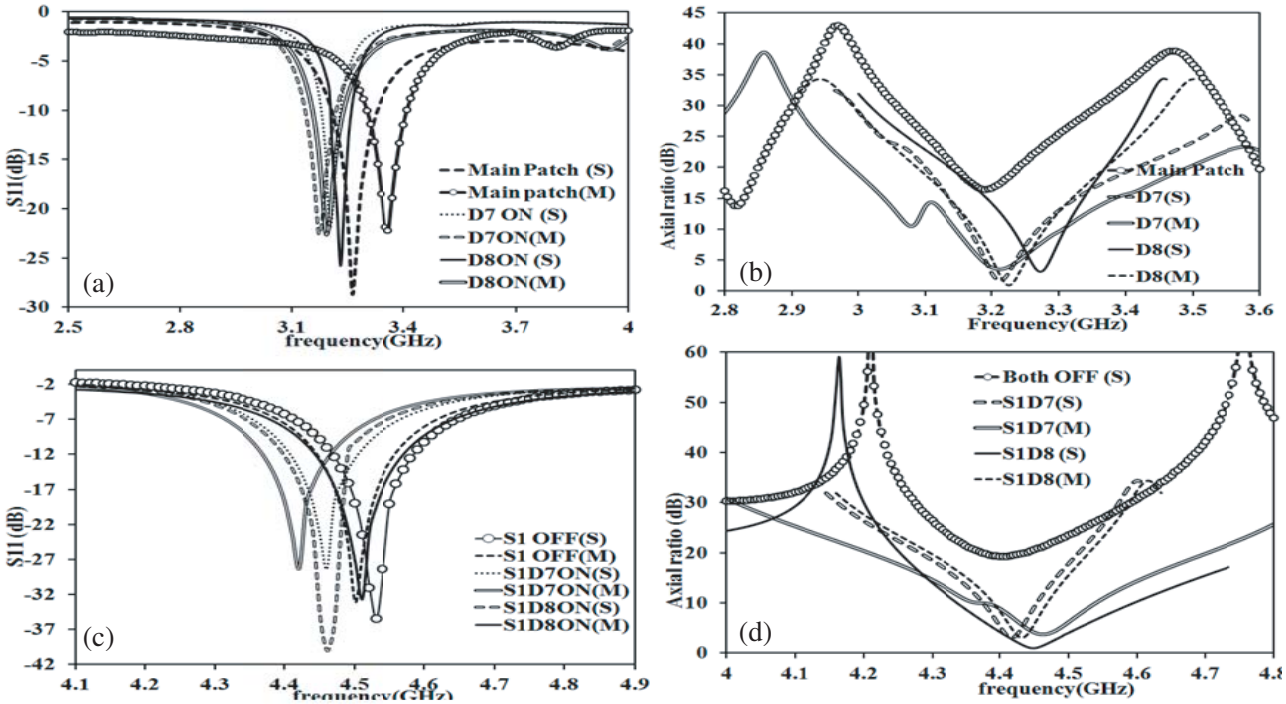

Figure 9. Simulated and measured S_{11} and axial ratio vs. freq. for (a)–(b) Case-A, (c)–(d) Case-B.

simulated and measured Axial Ratios (ARs) for Case-A. In this case when both diodes D_7 and D_8 are OFF, the main patch radiates a LP signal at 3.26 GHz. When either of the diodes D_7 or D_8 is ON, the antenna radiates CP signal. When diode D_7 is forward biased, the antenna shows an AR = 1.6 dB at 3.2 GHz. Similarly when diode D_8 is forward biased, the antenna shows an AR = 3.15 dB at 3.23 GHz. Figs. 9(a)–(b) show simulated and measured S_{11} vs. frequency for Case-A, and Figs. 9(c)–(d) show simulated and measured ARs vs. frequency for Case-B. In this case when diodes D_7 and D_8 are OFF, the main patch radiates an LP signal at 4.53 GHz. When diode D_7 is forward biased, the antenna shows an AR = 2.6 dB at 4.46 GHz. Similarly when diode D_8 is forward biased, the antenna shows an AR = 1.7 dB at 4.46 GHz.

3.4. Bandwidth Reconfigurable Mode

In this mode, antenna can reconfigure its operating bandwidth in either UWB mode or any NB by switching the active port state. The proposed antenna will work for UWB mode if port[1] is activated, and it can switch its bandwidth over any one of five NB (case[1]–case[5]) when port[2] is activated. This combination is important to attain the benefits of WB (multiple services simultaneously) and NB antennas in a single structure.

3.5. Pattern Reconfigurable Mode

It is an established fact that to realize pattern reconfiguration, direction of pattern should shift at constant resonant frequency. The shape and direction of radiation pattern strongly depends on current distribution in substrate along with the shape and size of radiating antenna. So, in this mode, direction of the pattern is shifted by changing the current distribution in the substrate without shifting the resonant frequency. To implement the concept of pattern reconfiguration in the proposed design, a U-shape parasitic arc is designed which encloses the main patch at a distance of 5.5 mm as shown in Fig. 10(a). The dimensions for parasitic arc are $W_R = 28.5$ mm, $L_R = 54.4$ mm. Two PIN diodes D_9 and D_{10} are used to short the arc at two points, 'A' and 'B'. As shorting points 'A' and 'B' are not directly attached with the active antenna and symmetrically placed in parasitic arc, the resonant frequency does not shift. But by shorting the parasitic arc, E-field distribution in the antenna is disturbed which results in shift of direction and shape of radiation pattern. To short the arc at point 'A' diode D_9 is activated by giving +5 V on V_8 DC bias pad and ground signal on V_{gd} bias pad. Similarly to short the arc at point 'B' diode D_{10} is activated through V_8 and V_{gd} DC pads.

The presence of short on the parasitic ring results in reformation of the electric field distribution leading to a shift of the main beam direction away from the short position. Three cases are studied using different conditions of diodes D_9 and D_{10}. In all cases, change in the direction of the beam is defined by the combined effect of location of short at the parasitic arc and basic radiation pattern of main patch in an ideal case. Generally, a null appears opposite to the position where the short is placed,

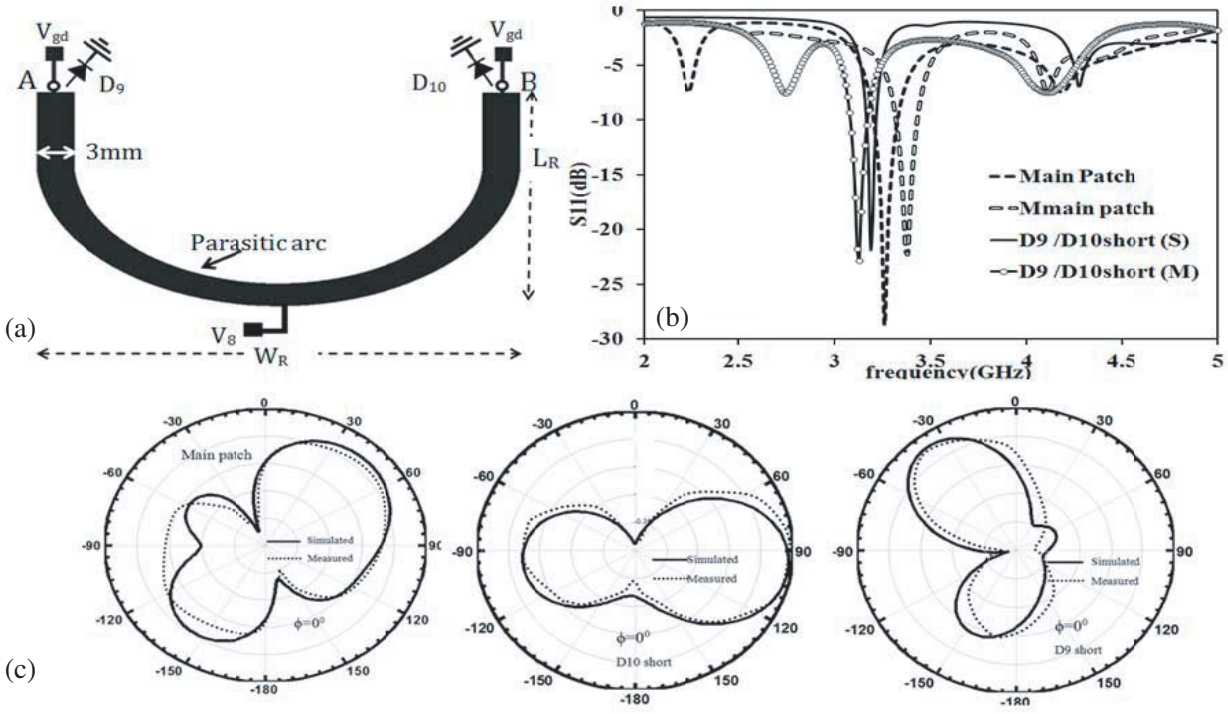

Figure 10. (a) Layout of parasitic arc, (b) simulated and measured S_{11} vs. freq., (c) observed E plane for all the cases.

but due to uneven distribution of the electric fields by the various components the antenna can radiate in any direction with any shape. As diodes D_9 and D_{10} are symmetrically placed in parasitic arc, there is no pronounced shift in resonant frequency. So the return loss behavior for one diode condition is shown here. For pattern reconfiguration resonant frequency should be constant, but pattern should reconfigure its direction and shape around that frequency. Fig. 10(b) shows the simulated and measured S_{11} vs. frequency when either of diode D_9 or D_{10} is shorted. The observed resonant frequency is nearly 3.26 GHz constant for all the cases. The observed E-plane radiation patterns for all the cases are given in Fig. 10(c).

4. CONCLUSION

The proposed antenna is versatile in nature as it can reconfigure its polarization state, resonant frequency and radiation pattern as well. The integration of UWB and reconfiguration antenna features solves the problem in requirement of multiple antennas or space, so it adds versatility to the antenna solution for CR systems. This approach may be useful in designing multimode wireless terminals while keeping the required antenna footprint small. For integration, large printed area of UWB monopole is used as a ground plane for designing second antenna. The integration concept is based on sharing some sections of one antenna between several other antennas without interfering with each other. A printed UWB antenna is selected as the main antenna, and then a reconfigurable antenna is integrated on the partially etched ground plane of a UWB antenna. So, there is efficient reutilization of printed space as two independent antennas are printed on a single substrate.

REFERENCES

1. Mansoul, A., F. Ghanem, M. R. Hamid, and M. Trabelsi, "A selective frequency-reconfigurable antenna for cognitive radio applications," *IEEE Antennas and Wireless Propag. Lett.*, Vol. 13, 515–518, 2014.
2. Sharma, S., C. C. Tripathi, and R. Rishi, "Cognitive radio: An efficient and effective solution for future spectrum implications," *IEEE International Conference on Computer, Communications and Electronics (Comptelix 2017)*, Jaipur, India, Jul. 1–2, 2017.
3. Tawk, Y., M. Bkassiny, G. El Howayek, et al., "Reconfigurable front-end antennas for cognitive radio applications," *IET Microw. Antennas Propag.*, Vol. 5, No. 8, 985–992, 2011.
4. Ebrahimi, E., J. R. Kelly, and P. S. Hall, "Integrated wide-narrowband antenna for multi-standard radio," *IEEE Trans. Antennas Propag.*, Vol. 59, No. 7, 2628–2635, 2011.
5. Manteghi, M. A., "Switch-band antenna for SDR applications," *IEEE Antennas Wireless Propag. Lett.*, Vol. 8, 3–5, 2009.
6. Sharma, S. and C. C. Tripathi, "Wideband to concurrent tri-band frequency reconfigurable microstrip patch antenna for wireless communication," *International Journal of Microwave and Wireless Technologies*, Vol. 9, No. 4, 915–922, 2017.
7. Hamid, M. R., P. Gardner, P. S. Hall, and F. Ghanem, "Vivaldi antenna with integrated switchable band pass resonator," *IEEE Trans. Antennas Propag.*, Vol. 59, No. 11, 4008–4015, 2011.
8. Qin, P. F., F. Wei, and Y. Jay Guo, "A wideband-to-narrowband tunable antenna using a reconfigurable filter," *IEEE Trans. Antennas Propag.*, Vol. 63, No. 5, 2282–2285, 2015.
9. Aboufoul, T., A. Alomainy, and C. Parini, "Reconfiguring UWB monopole antenna for cognitive radio applications using GaAs FET switches," *IEEE Antennas and Wireless Propag. Lett.*, Vol. 11, 392–395, 2012.
10. Sharma, S. and C. C. Tripathi, "A novel reconfigurable antenna with separate sensing mechanism for CR system," *Progress In Electromagnetics Research C*, Vol. 72, 187–196, 2017.
11. Sharma, S. and C. C. Tripathi, "An integrated frequency reconfigurable antenna for cognitive radio application," *Radioengineering*, Vol. 26, No. 3, 746–754, 2017.

12. Augustin, G. and T. A. Denidni, "An integrated ultra wideband/narrow band antenna in uniplanar configuration for cognitive radio systems," *IEEE Trans. Antennas Propag.*, Vol. 60, No. 11, 5479–5484, 2012.
13. Erfani, E., J. Nourinia, C. Ghobadi, and M. Niroo-Jazi, "Design and implementation of an integrated UWB/reconfigurable-slot antenna for cognitive radio applications," *IEEE Antennas and Wireless Propag. Lett.*, Vol. 11, 77–80, 2012.
14. Sharma, S. and C. C. Tripathi, "A wide spectrum sensing and frequency reconfigurable antenna for cognitive radio," *Progress In Electromagnetics Research C*, Vol. 67, 11–20, 2016.
15. Sharma, S. and C. C. Tripathi, "A versatile reconfigurable antenna for cognitive radio," *Asia Pacific Microwave Conference, APMC-2016*, New Delhi, India, Dec. 5–9, 2016.
16. Sharma, S., C. C. Tripathi, and R. Rishi, "A versatile reconfigurable antenna with integrated sensing mechanism," *International Journal of Microwave and Wireless Technologies*, Vol. 10, No. 4, 469–478, 2018.
17. Hussain, R. and M. S. Sharawi, "A cognitive radio reconfigurable MIMO and sensing antenna system," *IEEE Antennas and Wireless Propag. Lett.*, Vol. 14, 257–260, 2015.
18. Sharma, S., C. C. Tripathi, and R. Rishi, "Impedance matching techniques for microstrip patch antenna," *Indian Journal of Science and Technology*, Vol. 10, No. 28, 1–16, Jul. 2017.